

## Flux-lattice melting in layered superconductors

R. Šášík and D. Stroud

*Department of Physics, The Ohio State University, Columbus, Ohio 43210*

(Received 24 June 1993)

We describe a new representation to treat flux-lattice melting in an extreme type-II layered superconductor, generalizing an approach of Hu and MacDonald. The Ginzburg-Landau free-energy functional is expanded in eigenstates which are products of the lowest Landau levels in the  $xy$  plane, and tight-binding Bloch states in the  $z$  direction. The various correlation functions can be evaluated efficiently by Monte Carlo simulations. The melting temperature for a model of  $\text{Bi}_2\text{Sr}_2\text{CaCu}_2\text{O}_{8+\delta}$ , as estimated from the apparently simultaneous disappearance of Bragg peaks in the density-density correlation function, and of long-range interlayer correlations, is estimated to be about 30 K at a field of 1 T, in reasonable agreement with the experimental value of 26 K.

The standard Abrikosov<sup>1</sup> picture of type-II superconductors has to be modified in the CuO-based high-temperature superconductors. Instead of triangular flux lattice which persists up to the upper critical field  $H_{c2}(T)$ , there is a broad region in the  $H$ - $T$  plane occupied by a "melted flux liquid."<sup>2</sup> In this region, the flux lines are mobile, giving rise to a vortex structure with no long-range spatial order and with a finite resistivity. The prominence of the flux-liquid phase is thought to be due to large thermal fluctuations arising from the extremely small coherence lengths and high anisotropy in the high- $T_c$  materials. Many workers have calculated this melting line,<sup>2,3</sup> while other investigations have focused on how the melting transition is modified by defects.<sup>4</sup>

Recently, Hu and MacDonald<sup>5</sup> have developed a novel order-parameter expansion to describe flux-lattice melting in two-dimensional (2D) superconductors. They expand the Ginzburg-Landau order parameter  $\psi$  in Landau levels, and retain only the lowest Landau level. Their formalism allows both the quadratic and quartic terms in the Ginzburg-Landau free-energy functional to be expressed compactly. The various correlation functions and transition temperature can then be accurately determined by Monte Carlo methods.

In this paper, we extend this method to 3D layered superconductors. We start from a Ginzburg-Landau functional in which the mean-field transition temperature  $T_{c0}(z)$  is periodic in  $z$ , the  $c$ -axis coordinate. When the applied field  $\mathbf{H} \parallel \hat{z}$ ,  $\psi(\mathbf{r})$  is conveniently expanded in eigenstates which are products of Landau levels in the  $xy$  plane and Bloch states in the  $z$  direction. For highly anisotropic high- $T_c$  superconductors, it suffices to include just the lowest Bloch band, and to treat this within the nearest-neighbor tight-binding approximation. We then find, just as in the 2D case, that both the quadratic and quartic terms have convenient analytical expressions within which Monte Carlo simulations can be performed. The basis is composed of the states in the lowest Landau level of each layer.

The resulting formalism is nearly assumption independent, in that nearly all the parameters can be determined from experiment. In particular, the width of the lowest Bloch band follows directly from the measured effective mass ratio. A quartic matrix element which enters the

theory depends on the Wannier function for the lowest band, and hence on the assumed analytic form of  $T_{c0}(z)$ , but this dependence appears to be weak. Also, since the theory makes no explicit mention of vortex variables, the melting temperature and other properties of the vortex solid and liquid can be computed without having to consider the difficult question of flux-line cutting and reconnection.

We assume that the superconducting phase is described by a complex order parameter  $\psi(\mathbf{r})$  and a free-energy functional

$$F[\psi(\mathbf{r})] = \int d^3r [a(\mathbf{r})|\psi|^2 + \frac{1}{2}b|\psi|^4 + (2m)^{-1} \times |(-i\hbar\nabla - q\mathbf{A}(\mathbf{r})/c)\psi|^2 + |\mathbf{h}(\mathbf{r})|^2/8\pi], \quad (1)$$

where  $q = -2e$ . In the extreme type-II limit, we approximate the local field  $\mathbf{h}(\mathbf{r})$  by the applied field  $\mathbf{H}$ , and neglect fluctuations in the vector potential  $\mathbf{A}(\mathbf{r})$ . We consider  $\mathbf{H} = H\hat{z}$ , and assume  $a(\mathbf{r}) = \alpha[T - T_{c0}(z)]$ , where  $T_{c0}(z)$  is periodic with period  $d$ .  $\alpha$  and  $b$  are taken to be  $z$  independent.

We will expand  $\psi(\mathbf{r})$  in terms of solutions to the linearized Ginzburg-Landau equation

$$a(\mathbf{r})\psi(\mathbf{r}) + (2m)^{-1}(-i\hbar\nabla - q\mathbf{A}/c)^2\psi(\mathbf{r}) = 0. \quad (2)$$

With the gauge choice  $\mathbf{A} = -Hy\hat{x}$ , the solution to Eq. (2) may be expressed as a wave function of the form  $\psi(\mathbf{r}) = \Phi(x, y)\zeta(z)$ , where  $\Phi(x, y)$  and  $\zeta(z)$  are respectively eigenstates of the Hamiltonians  $H_{\perp} = (2m)^{-1}(-i\hbar\nabla_{\perp} - q\mathbf{A}/c)^2$  and  $H_{\parallel} = -\alpha T_{c0}(z) - (\hbar^2/2m)\nabla_{\parallel}^2$ .

The eigenstates of  $H_{\perp}$  are Landau levels. As discussed in Ref. 5, it is sufficient, in the low screening limit, to expand the free-energy functional in the lowest Landau level only. The corresponding wave function may be written  $\Phi_{k_x}(x, y) = e^{ik_x x} \varphi_0(y - y_{k_x})$ , where  $\varphi_0(y) = (\beta^2/\pi)^{1/4} \exp(-\beta^2 y^2/2)$ ,  $\beta^2 = |q|H/(\hbar c)$ , and  $y_{k_x} = k_x/\beta^2$ . The frequency corresponding to this harmonic oscillator wave function is  $\omega_c = |q|H/(mc)$ .

Since  $T_{c0}(z)$  is periodic with period  $d$ , the eigenstates of  $H_{\parallel}$  are Bloch states. We assume that only the lowest band enters into the free energy, and furthermore, can be represented as a tight-binding band with only

nearest-neighbor hopping (this will be justified below). The eigenfunctions  $\zeta(z)$  can be written  $\zeta_{k_x}(z) = \sum_n u(z-nd)\exp(ik_z nd)$ , where  $u(z-nd)$  is the (properly orthonormalized) Wannier function for the lowest band in the  $n$ th layer. The corresponding energy is  $E(k_z) = E_0 - 2t \cos(k_z d)$ , where  $t$  is the tight-binding matrix element.

Expanding the order parameter as

$$\psi(\mathbf{r}) = \sum_{k_x, n} c_{k_x, n} \Phi_{k_x}(x, y) u(z-nd), \quad (3)$$

and substituting into Eq. (1), we obtain, omitting the nonfluctuating field energy,  $F = F^{(2)} + F^{(4)}$ , where

$$F^{(2)} = L_x \sum_{k_x, n} |c_{k_x, n}|^2 \left( \frac{1}{2} \hbar \omega_c + E_0 + \alpha T \right) - L_x t \sum_{k_x, n} c_{k_x, n} (c_{k_x, n+1}^* + c_{k_x, n-1}^*), \quad (4)$$

$$F^{(4)} = \frac{L_x b \beta}{\sqrt{8\pi}} u_{0000} \sum_{k_x, n, q_1, q_2} c_{k_x, n} c_{k_x+q_1, n}^* c_{k_x+q_2, n}^* \times c_{k_x+q_1+q_2, n} V(q_1, q_2) + \dots \quad (5)$$

Here  $V(q_1, q_2) = \exp[-(q_1^2 + q_2^2)/2\beta^2]$  and  $u_{0000} = \int_{-\infty}^{\infty} |u(z)|^4 dz$ . The ellipses in Eq. (5) denote higher-order terms, involving products of four Wannier functions from more than one layer. We retain only the diagonal part of the fourth-order term, i.e., the first term of expansion (5), corresponding to four-wave mixing of Landau states only in the same layer. Interlayer coupling is still generated by the quadratic term. The normalization in Eqs. (4) and (5) is chosen for convenience so that the resulting coefficients  $c_{k_x, n}$  are independent of sample size.

The sample is assumed to be a parallelepiped of dimension  $L_i$  in the  $i$ th direction.

The parameters of this model can easily be connected to measurable parameters of real materials. First, the mean-field transition temperature  $T_{c0}(H)$  is given by the lowest eigenvalue of the linearized Ginzburg-Landau equation (2), i.e.,  $-\alpha T_{c0}(H) = \frac{1}{2} \hbar \omega_c + E_0$ . Writing  $T_{c0}(H) = T_{c0}(0) - H / |dH_{c2}/dT|_{T=T_{c0}(0)}$ , we can identify  $E_0 = -(\hbar|q|/2mc) T_{c0}(0) |dH_{c2}/dT|_{T=T_{c0}(0)}$ , and  $\alpha = (\hbar|q|/2mc) |dH_{c2}/dT|_{T=T_{c0}(0)}$ . Similarly, the quartic coefficient  $b$  can be expressed in terms of the Ginzburg-Landau parameter  $\kappa \equiv \lambda_1/\xi_1$  (where  $\xi_1$  and  $\lambda_1$  are the transverse correlation length and penetration depth), via the relation<sup>6</sup>  $b = 2\pi\kappa^2(\hbar|q|/mc)^2$ . Finally, we can define the longitudinal effective mass  $m_{\parallel}$  in terms of the tight-binding integral by

$$\frac{\hbar^2}{2m_{\parallel}d^2} \equiv \frac{1}{2d^2} \left[ \frac{\partial^2 E(k_z)}{\partial k_z^2} \right]_{k_z=0} = t = \frac{\hbar^2}{2gmd^2}, \quad (6)$$

where we have introduced the mass ratio  $g = m_{\parallel}/m$ . Since  $g$  can be inferred from induced torque measurements,<sup>7</sup> this equation expressed  $t$  entirely in terms of measurable quantities.

We have studied this model using parameters appropriate to  $\text{Bi}_2\text{Sr}_2\text{CaCu}_2\text{O}_{8+\delta}$ :  $T_{c0}(0) = 86$  K,

$|dH_{c2}/dT|_{T=T_{c0}(0)} = 5100$  Oe K<sup>-1</sup>,  $d = 30.9$  Å,  $g = (55)^2$  and  $\kappa \approx 100$ . To estimate  $u_{0000}$ , we use a simple model, based on the expectation that  $T_{c0}(z)$  is sharply peaked within the paired CuO layers in  $\text{Bi}_2\text{Sr}_2\text{CaCu}_2\text{O}_{8+\delta}$ . If we make the simple Kronig-Penney approximation  $T_{c0}(z) \approx \tau_0 + \tau \sum_{n=-\infty}^{\infty} \delta(z-nd)$ , the delta function has one bound state  $u(z) = (1/\sqrt{z_0}) \exp(-|z|/z_0)$ , where  $z_0 = \hbar^2/(m\alpha\tau)$ . The corresponding  $u_{0000} = 1/(2z_0)$ . The overlap integral is then readily expressed in terms of  $z_0$  using the relation  $t = (\hbar^2/mz_0^2) \exp(-d/z_0)$ . Combined with Eq. (6) for  $t$ , this equation gives  $(z_0/d)^2 \exp(d/z_0) = 2g$ , from which  $u_{0000}$  can be readily calculated. Using the parameters given above, one obtains  $t/E_0 = 0.00025$ ;  $z_0/d = 0.07$ , validating the nearest-neighbor tight-binding assumption for this material. Although our choice of  $T_{c0}(z)$  may seem arbitrary, we believe that  $u_{0000}$  will be insensitive to this choice, depending mainly on the range  $z_0$  of the Wannier function, and hence on  $g$ . Note also that the matrix element never really enters the theory by itself, but only in the a combination  $bu_{0000}$ .

We describe our numerical results in terms of the two-point correlation function

$$\Gamma^{(2)}(\mathbf{r}, \mathbf{r}') \equiv \langle \psi(\mathbf{r}) \psi^*(\mathbf{r}') \rangle, \quad (7)$$

and the density-density correlation function

$$\Gamma^{(4)}(\mathbf{r}, \mathbf{r}') \equiv \langle |\psi(\mathbf{r})|^2 |\psi(\mathbf{r}')|^2 \rangle \quad (8)$$

where the brackets denote a canonical average. The relevant Fourier transforms are  $\Gamma^{(p)}(\mathbf{q}_1, \mathbf{q}_2) = \int d\mathbf{r}_1 d\mathbf{r}'_1 dz dz' \exp[i\mathbf{q}_1 \cdot (\mathbf{r}_1 - \mathbf{r}'_1) + i\mathbf{q}_2 \cdot (z - z')] \Gamma^{(p)}(\mathbf{r}, \mathbf{r}')$ , where  $p = 2$  or  $4$ . These expressions can be rewritten in terms of the coefficients  $c_{k_x, n}$ , with the results

$$\Gamma^{(2)}(q_x, 0, 0) = G_{\text{at}}^{(2)}(q_x) \frac{d}{L_x L_y L_z} \sum_{k_x, n} \langle c_{k_x+q_x, n} c_{k_x, n}^* \rangle, \quad (9)$$

where  $G_{\text{at}}^{(2)}(q_x) = (L_y L_z / d) \exp(-q_x^2 / 4\beta^2)$  is an atomic form factor;

$$\Gamma^{(4)}(q_x, 0, 0) = G_{\text{at}}^{(4)}(q_x) \left\langle \left| \frac{d}{L_x L_y L_z} \sum_{k_1, n} c_{k_1, n} c_{k_1+q_x, n}^* \right|^2 \right\rangle, \quad (10)$$

where  $G_{\text{at}}^{(4)} = (G_{\text{at}}^{(2)}(q_x))^2$ .

We choose a sample cell commensurate with the Abrikosov ground state:  $L_x = n_x l_0$  and  $L_y = n_y (\frac{1}{2}\sqrt{3}l_0)$ , where  $n_x$  and  $n_y$  are integers, and  $l_0 = (4\pi/\beta^2\sqrt{3})^{1/2}$  is the spacing between nearest-neighbor vortices. The allowed set of  $k_x$  indices is then  $k_x = 2\pi p / L_x$ , where  $p = 0, 1, \dots, N_\phi - 1$  and  $N_\phi/n_x$  is an even integer  $n_y$ . The resulting  $L_x \times L_y$  rectangle can accommodate  $N_\phi$  flux lines, arranged in  $n_y$  rows, each containing  $n_x$  vortices.

We have evaluated these correlation functions using a variant of the Metropolis Monte Carlo algorithm. Our Monte Carlo cell contains 56 vortices and holds 8 layers in the  $z$  direction. The dimensions of the cell are  $L_x = 7l_0$ ,  $L_y = 4\sqrt{3}l_0$ , and  $L_z = 8d$ , with periodic boundary conditions in all three directions. In our algorithm, a single Monte Carlo move consists of displacing *all* the

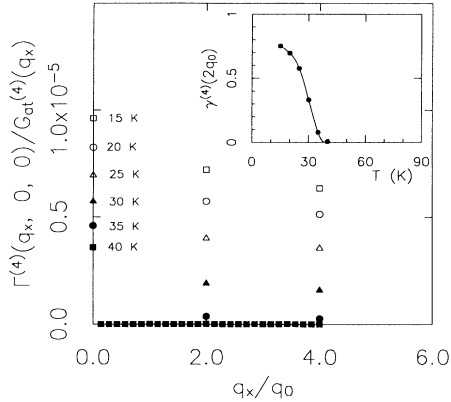


FIG. 1. Four-point correlation function or “structure factor”  $\Gamma^{(4)}(q_x, 0, 0)/G_{\text{at}}^{(4)}(q_x) \equiv \tilde{\Gamma}^{(4)}(q_x)$  for model  $\text{Bi}_2\text{Sr}_2\text{CaCu}_2\text{O}_{8+\delta}$ , in  $\text{cm}^{-6}$ , calculated at several temperatures  $T$  by Monte Carlo simulation at a field  $H=1.0 \times 10^4$  Oe. Inset:  $\gamma^{(4)}(2q_0) \equiv \tilde{\Gamma}^{(4)}(2q_0)/\tilde{\Gamma}^{(4)}(0)$ , plotted as a function of  $T$ . The wave-number scale is defined by  $q_0=2\pi/l_0$ , where  $l_0=[2\Phi_0/(\sqrt{3}H)]^{1/2}$  is the intervortex spacing, and  $\Phi_0=hc/q$  is the flux quantum.

amplitudes in a given layer. Because of the long-range interactions in  $k$  space within a plane, this approach seems to be comparably efficient to the more conventional approach of displacing each amplitude successively; and it clearly satisfies the requirements of ergodicity and microscopic reversibility. At each temperature, we start from the known Abrikosov state (this greatly speeds up the equilibration), equilibrate the ensemble by  $5 \times 10^4$  passes through the entire lattice, and evaluate the required averages over the next  $10^4$  passes. We have confirmed that this equilibration time is sufficient to produce approximately time-independent ensemble averages.

We have carried out preliminary calculations at a field  $H=1.0 \times 10^4$  Oe, and found evidence for a melting transition near  $T=30$  K, in reasonable agreement with the experimental value of 26 K.<sup>8</sup> Figure 1 shows the “structure factor”  $\Gamma^{(4)}(q_x, 0, 0)/G_{\text{at}}^{(4)}(q_x)$  as a function of  $q_x$  for several temperatures. [In this and all successive calculations, we use units such that  $\hbar|q|/(mc)=1$ . Note also that for this choice of direction, the Bragg peak corresponding to the shortest reciprocal lattice vector is not calculated.] The intensity of the sharp Bragg-like peaks

diminishes with increasing temperatures, presumably because of Debye-Waller factors associated with vibrations of the effective vortex lattice, and they disappear altogether above about 30 K, where the vortex lattice melts. The peak at  $q_x=0$  persists to  $\sim T_{c0}(H)$ . This is because this peak represents the presence of a finite *amplitude*, rather than a flux lattice with long-range phase coherence.

The two-point correlation function  $\Gamma^{(2)}(x, 0, 0)$  [Fig. 2(a)] shows oscillations with the periodicity of the crystal at low temperatures. Note the real-space peaks of Fig. 2(a) are *not* delta-functions, as are the analogous Bragg peaks for either the two-point or four-point correlation functions in reciprocal space. Also, in contrast to Fig. 1, we have retained the “atomic” form factors in making these real-space plots. The results for  $\Gamma^{(2)}(0, 0, nd)$  [Fig. 2(b)] are especially sensitive to the correlations *between* the planes. The finite saturation value at large separations probably indicates the onset of long-range phase coherence in the sample, i.e., long-range correlations in the phase  $\phi(\mathbf{r})$  of the order parameter  $\psi(\mathbf{r})=|\psi(\mathbf{r})|\exp(i\phi(\mathbf{r}))$ . The two-point correlation function will primarily reflect phase, rather than amplitude correlations, because the amplitude itself will not fluctuate very much at these temperatures, which are well below  $T_{c0}$ .

In Fig. 3, we show “snapshots” of the vortex configurations in a particular sample plane after  $5 \times 10^4$  passes and at temperatures  $T=20$  K [Fig. 3(a)] and 40 K [Fig. 3(b)]. The planes show evidence of a long-range triangular lattice at the lower temperature, which disappears at the higher temperature. The darkened areas shown within each figure represent the vortex cores of the same ensemble member four layers away. The pictures thus suggest [as do Figs. 2(a) and 2(b)] that the interlayer and intralayer correlations disappear near the same temperature.

As a check on our calculations, we have compared our results with the 2D calculations of Ref. 5. Their parameter  $g^2 \approx 43.5$  at melting, corresponding to a single-layer melting temperature of about 26 K for our system, if we assume a layer thickness of about  $2z_0$ . Our 3D melting at  $H=10^4$  Oe appears to occur at only a slightly higher temperature, presumably because the interlayer coupling is weak. (Even without any interlayer coupling, the transition temperature would be higher than 26 K for our

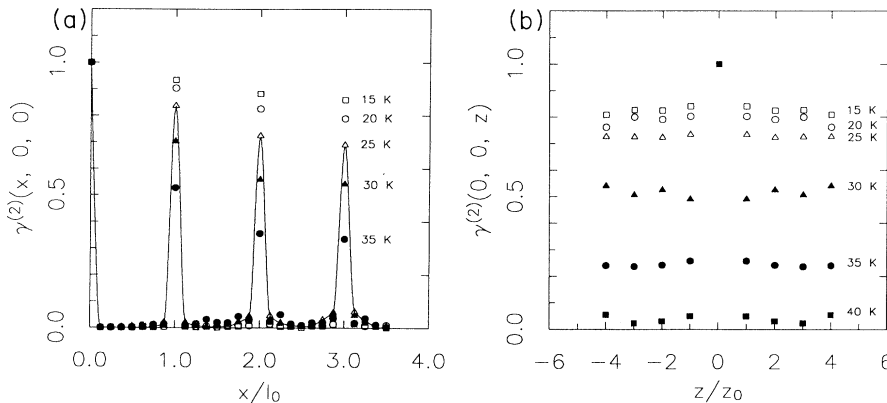


FIG. 2. (a) Normalized two-point correlation function  $\gamma^{(2)}(x, 0, 0) \equiv \Gamma^{(2)}(x, 0, 0)/\Gamma^{(2)}(0, 0, 0)$ , plotted as a function of  $x/l_0$  at several temperatures  $T$  for model  $\text{Bi}_2\text{Sr}_2\text{CaCu}_2\text{O}_{8+\delta}$ . (b) Normalized  $\gamma^{(2)}(0, 0, nd) \equiv \Gamma^{(2)}(0, 0, nd)/\Gamma^{(2)}(0, 0, 0)$  vs temperature.  $d$  is the interlayer separation. Solid line is merely to guide the eye at  $T=25$  K.

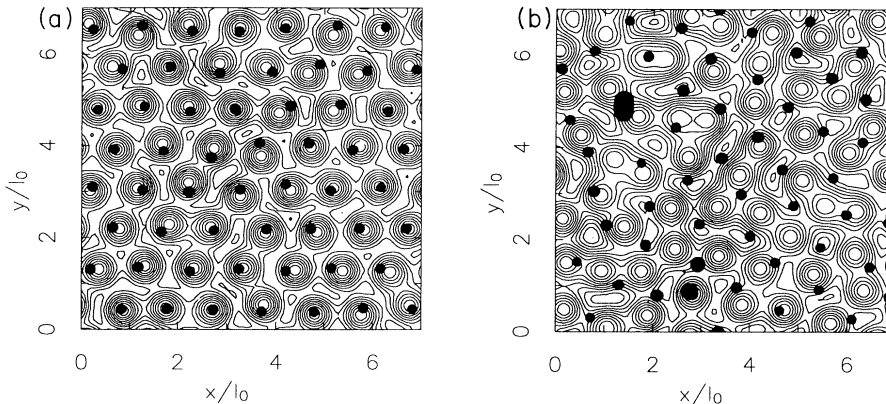


FIG. 3. Snapshots of the vortex configuration in the layer at  $z=0$  at (a)  $T=20$  K; (b)  $T=40$  K. The contour lines represent loci of constant  $|\psi|^2$ . Darkened areas denote normal regions (vortex cores) in a layer at  $z=4d$ . Note the overlapping vortex cores at 40 K.

small sample sizes.) Near 20 K, we estimate that the typical “phase flip” energy per pancake  $|4J_0tc_{k_x,n}c_{k_x,n+1}^*|$  is about 0.4 K. This energy is small but finite, which causes the ordering between planes to “freeze” at the same temperature as the 2D pancakes within planes. The interplane interaction energy [the second term of Eq. (8)], which averages to zero due to phase disorder in the vortex liquid state, suffers a discontinuous and thermodynamically extensive change upon 2D ordering, thus causing the simultaneous onset of phase coherence between planes. We conjecture that this model Hamiltonian has a single phase transition in this geometry, in agreement with experiments,<sup>7</sup> while the question whether there is a double transition in tilted magnetic field remains open.

It would be of great interest to know if this flux lattice melting transition is first-order or continuous. Recent computer simulations based on a stacked triangular lattice of XY spins<sup>9</sup> strongly suggest a first-order transition, as do experiments on  $\text{YBa}_2\text{Cu}_3\text{O}_{7-\delta}$ .<sup>10</sup> The 2D version of the present model has a first-order transition.<sup>5</sup> Although our numerical evidence is inconclusive, a simplistic analytical argument suggests a first-order 3D melting transition. In the ordered state,  $|\psi(\mathbf{r})|^2$  has nonzero Fourier components at the reciprocal lattice vectors of a

stacked triangular lattice. The shortest of these lies in the  $xy$  plane and has magnitude  $4\pi/(\sqrt{3}l_0)$ . Since there exist sets of three such shortest vectors summing to zero, it follows, by well-known arguments,<sup>11</sup> that a Ginzburg-Landau theory using the amplitudes of these Fourier components as order parameters has a cubic term, and therefore, a *first-order* transition. (This argument would also predict a first-order transition in the single-layer case.)

The present approach has a number of other possible applications, e.g., to systems which contain various types of pinning centers. Likewise, it would be straightforward to treat magnetic fields which have a component parallel to the  $ab$  plane, and hence, to seek the double transition reported in this geometry.<sup>8</sup> Finally, as has been done by other authors using quite different representations,<sup>12,13</sup> it would, of course, be desirable to extend these Monte Carlo calculations to treat *dynamical* properties.

This work has been supported by NSF Grant No. DMR90-20994, and by the Midwest Superconductivity Consortium (MISCON) at Purdue University, through DOE Grant No. DE-FG02-90ER45427. Calculations were carried out on the Cray Y-MP 8/8-64 of the Ohio Supercomputer Center.

<sup>1</sup>A. A. Abrikosov, Zh. Eksp. Teor. Fiz. **32**, 1442 (1957) [Sov. Phys. JETP **5**, 1174 (1957)].

<sup>2</sup>D. R. Nelson, Phys. Rev. Lett. **60**, 1973 (1988); M. C. Marchetti and D. R. Nelson, Phys. Rev. B **41**, 1910 (1990); Lei Xing and Z. Tešanović, Phys. Rev. Lett. **65**, 794 (1990); A. Houghton, R. A. Pelcovits, and A. Sudbø, Phys. Rev. B **40**, 6763 (1989); S. Ryu *et al.*, Phys. Rev. Lett. **68**, 710 (1992).

<sup>3</sup>Y. Li and S. Teitel, Phys. Rev. Lett. **66**, 3301 (1991); S. Sengupta *et al.*, *ibid.* **67**, 3444 (1991); J. R. Clem, Phys. Rev. B **43**, 7837 (1991).

<sup>4</sup>See, e.g., D. S. Fisher, M. P. A. Fisher, and D. A. Huse, Phys. Rev. B **43**, 130 (1991).

<sup>5</sup>Jun Hu and A. H. MacDonald, Phys. Rev. Lett. **71**, 432 (1993).

<sup>6</sup>P. G. de Gennes, *Superconductivity of Metals and Alloys* (Addison-Wesley, New York, 1989), p. 181.

<sup>7</sup>D. E. Farrell *et al.*, Phys. Rev. Lett. **63**, 782 (1989).

<sup>8</sup>C. Duran *et al.*, Phys. Rev. B **44**, 7737 (1991).

<sup>9</sup>R. A. Hetzel, A. Sudbø, and D. A. Huse, Phys. Rev. Lett. **69**, 518 (1992).

<sup>10</sup>H. Safar *et al.*, Phys. Rev. Lett. **69**, 824 (1992).

<sup>11</sup>S. Alexander and J. McTague, Phys. Rev. Lett. **41**, 702 (1978).

<sup>12</sup>S. Ryu, S. Doniach, and A. Kapitulnik (unpublished).

<sup>13</sup>K. H. Lee, D. Stroud, and S. M. Girvin, Phys. Rev. B **48**, 1233 (1993).